

Identification of the cell wall proteins associated with the softening of *Lycium barbarum* L. fruit by using iTRAQ technology

Jun Liu^a, Qin Ma^b, Dunhua Liu^{a,b,*}, Caixia Meng^b, Ziying Hu^b, Lu Ma^c

^a School of Agriculture, Ningxia University, 750021 Yinchuan, People's Republic of China

^b School of Food & Wine, Ningxia University, 750021 Yinchuan, People's Republic of China

^c Department of Business Management, Shizuishan Institute of Industry and Trade, 753000 Shizuishan, People's Republic of China

ARTICLE INFO

Keywords:

Lycium barbarum L.
iTRAQ
Softening
Cell wall
RT-PCR

ABSTRACT

Excessive softening of *Lycium barbarum* L. (LBL) fruit can limit the storage and transportation of fresh fruit. To better understand the underlying molecular mechanisms of fruit softening in LBL, changes in the pre-climacteric (S1) and post-climacteric (S2) proteomes were investigated by iTRAQ methods. The 14-fold reduction in S2 fruit firmness compared to S1 was accompanied by increased respiratory intensity and degradation of cell wall components. A total of 258 differentially expressed proteins (DEPs) were identified, which were mainly associated with photosynthesis, carbohydrate, amino acids and fatty acids metabolism. From the functional proteomic analysis, enhanced energy metabolisms, such as glycolysis/gluconeogenesis and citrate cycle (TCA cycle) contributed to cell wall degradation and conversion to substrates for respiratory metabolism, leading to fruit softening. These findings have provided new insights into the molecular pathways associated with fruit softening in LBL and the bioinformatics analyses provided insightful information for further transcriptional studies.

1. Introduction

Lycium barbarum L. (LBL) is a typical melting flesh fruit that undergoes rapid ripening prior to harvest. Unfortunately, this softening is negative for the LBL and can reduce the nutritional and sensory qualities of the fruit (Liu et al., 2020, 2021; Liu, Liu, Li, & Zhao, 2020). The characteristics of fruit softening differ among species and cultivars, and are largely determined by cell wall modifications that are generally attributed to the disassembly of the cellulose and hemicellulose network through depolymerization of pectin and hemicellulose (Chea et al., 2019). The fruit cell wall is composed of cellulose, non-cellulosic wall polysaccharide polymers, such as hemicellulose and pectin, and a small amount of protein (Bashline, Lei, Li, & Gu, 2014). Hemicellulose attaches to cellulose microfibrils, forming the cellulose-matrix network that, together with lignin, gives the rigidity and strength to the cells. These cell wall components are synthesized at different locations and are assembled into a functional cell wall matrix that structurally supports cells and fruit (Xiao, Li, Jiang, Jiang, & Duan, 2019). The structure of the cell wall is required not only to be strong and rigid to provide the structural support for the fruit, but also to allow anisotropic cell expansion in a controlled manner. Therefore, various cell wall modifying enzymes and proteins are responsible for cell wall modifications

during the ripening and softening of fruits, including polygalacturonase (PG), pectin methylesterase (PME), pectate lyase (PL), α -arabinofuranosidase (AF), β -galactosidase (GAL), α -mannosidase, β -xylosidase and *endo*-1,4- β -xylanase (Defilippi, Ejsmentewicz, Covarrubias, & Gudenschwager, 2018; Goulao & Oliveira, 2008). Transcription factor-mediated regulation of softening-related gene expression is also involved in fruit softening (Gwanpua, Verlinden, Hertog, Nicolai, & Geeraerd, 2017). Thus, fruit softening is the result of cell wall modification caused by multiple factors, and the knowledge of cell wall mechanisms associated with these changes is fundamental for understanding how the cells control softening through cell wall synthesis and cell wall remodeling.

Given the complexity of the softening process, the use of tools that may allow an all-around evaluation of the molecular processes triggered within the fruit is important (Ricardo, Campos-Vargas, & Orellana, 2012). Proteomics may represent a prospective approach to revealing the complex physiological processes associated with fruit softening at the global protein level. An efficient and reliable quantitative method, isobaric tags for relative and absolute quantitation (iTRAQ), has been widely used for proteomic studies and facilitating more reproducible quantification and comprehensive elucidation of protein expression in an extremely complex biological system (Jiang, Kang, Feng, Yu, & Luo,

* Corresponding author at: No. 489, Mount Helan West Road, Xixia District, Yinchuan City, 750000 Ningxia Hui Autonomous Region, China.

E-mail addresses: dunhualiu@126.com, ldh320@nxu.edu.cn (D. Liu).

<https://doi.org/10.1016/j.fochms.2022.100110>

Received 3 February 2022; Received in revised form 22 April 2022; Accepted 2 May 2022

Available online 6 May 2022

2666-5662/© 2022 The Author(s). Published by Elsevier Ltd. This is an open access article under the CC BY-NC-ND license (<http://creativecommons.org/licenses/by-nc-nd/4.0/>).

2020). Recently, iTRAQ approaches have been generally used to explore the molecular mechanism underlying fruit ripening or softening in a range of species, including oriental melon (Guo, Xu, Cui, Chen, & Qi, 2017), *Vitis vinifera* (Martínez-Esteso, Vilella-Antón, Pedreo, Valero, & Bru-Martínez, 2013) and pomegranate (Niu et al., 2018), leading to the characterization of proteins, enzymes, and physiological regulatory networks associated with ripening and softening. These studies have, however, mainly focused on multiple ripening and softening-related processes, no single process such as fruit softening caused by cell walls. Currently, the cell wall proteome has been studied in several fruit species, including *Pyrus sinkiangensis* Yu (Gong et al., 2020), banana (Xiao et al., 2019), *Vitis vinifera* (Martínez-Esteso et al., 2009). Limited information about the cell wall proteome concerning LBL fruit softening is available, and the cell wall proteomic approach has been generally recognized as a powerful tool for elucidating complex characteristics of fruit development, paving the way for its application in LBL.

In the study, a comparative proteomic analysis by iTRAQ technology was performed to investigate the differential expressed cell wall proteins between the pre-climacteric (S1) and post-climacteric (S2) stages. The study aimed to identify the biochemical processes associated with the softening process and proteins that may play important roles in the softening process of LBL fruit. This study presented the first cell wall proteome of LBL fruit, based on detailed proteomic data. We have also provided new insights into the dynamics of protein abundance changes, contributing to further understanding of the molecular mechanisms underlying regulation of softening-related genes.

2. Materials and methods

2.1. Fruit collection

Lycium barbarum L. (LBL) (Ningqi 1) fruit samples were obtained from a fruit orchard at the sixth team plantation of Helan Mountain Farm in Ningxia, China. We collected fruit from 20 trees (more than 10 years old), and approximately 50 fruits per tree, with about 1000 fruits per period, which were mixed well in perforated LE-PE self-sealing bags. LBL was harvested in the morning and transported to the College of Agriculture, Ningxia University within 1 h after harvesting for the measurement of the fresh fruit firmness, respiration rate, and observation of the cell microstructure. Three portions of 50 g each of fruit from both stages of ripening were taken, frozen in liquid nitrogen, then stored at $-80\text{ }^{\circ}\text{C}$ for the extraction of cell wall components and proteins.

2.2. Measurements of physiological parameters

Firmness was determined in 10 individual fruits on the lumbar side of the fruit using a TA.XT Plus firmness tester (Stable Micro Systems Manufacturing Co., London, UK) (Ren et al., 2020).

The respiration rate of fruit was determined using a fruit and vegetable respirometer (SYS-GH30A, Saiyas Technology Co., Dandong, China). Briefly, the respiration intensity meter was switched on and preheated for 30 min at room temperature ($25\text{ }^{\circ}\text{C}$), 30 g of LBL was placed in a 0.25 L cylindrical respiration chamber and the gas circulation pump was switched on; zeroed and the value x_1 was recorded when the value was stable and x_2 after 5 min. The respiration rate was calculated as follows.

$$\text{Respiration rate [mg} \times (\text{kg} \cdot \text{h})] = \frac{(x_2 - x_1) \times 0.25 \times 44 \times 1000 \times 60}{v \times m \times 5}$$

where: x_1 , starting concentration of CO_2 phase, $\mu\text{mol/mol}$; x_2 , ending concentration of CO_2 phase, $\mu\text{mol/mol}$; 0.25, volume of cylindrical breathing chamber, L; 44, molar mass of CO_2 , g/mol; 24.45, molar volume of CO_2 at $25\text{ }^{\circ}\text{C}$, L/mol; m is the weight of the fruit used for the determination, kg; 1000, 60 and 5 are conversion factors.

Cell wall components were isolated in the form of alcohol-insoluble

residue as described previously. Isolated cell wall components were fractionated into water-soluble pectins (WSP), CDTA-soluble pectins (ISP), Na_2CO_3 -soluble pectins (CSP), KOH-soluble polymers (hemicelluloses) and H_2SO_4 -soluble polymers (celluloses) (Chea et al., 2019). Uronic acid contents in WSP, ISP and CSP fractions were determined by the them-hydroxy diphenyl method using galacturonic acid as a standard (Blumenkrantz & Asboe-Hansen, 1973). Hemicellulose and cellulose contents were measured using the anthrone method (D'Amour, Gosselin, Arul, Staigne, & Willemot, 2006) with glucose as a standard. The contents of galacturonic acid and glucose were measured using an UV-T6 spectrophotometer (Persee General Instruments Co., Ltd, Beijing, China).

2.3. Transmission electron microscopy (TEM)

Sample preparation of LBL for TEM was performed according to the method described by He et al. (2017). LBL flesh at the waist from the skin to endocarp was cut into slices of $3\text{ mm} \times 2\text{ mm}$. For TEM observations, all sections were examined under a H-7650 transmission electron microscope (Hitachi, Ltd. Tokyo, Japan) at 80 kV, and whole images were acquired.

2.4. Extraction of cell wall proteins

Cell wall proteins were extracted according to Xiao et al. (2019) with some modifications. Briefly, the samples of frozen LBL fruit tissue were finely powdered in liquid nitrogen and suspended sequentially with different concentrations of sucrose (0.4, 0.6 and 1.0 M) in ice-cold homogenizing acetate buffer (5 mM, pH 4.6) with mild stirring for 15 min. After each suspension, the mixture was centrifuged and the supernatant was then discarded. The grain was washed twice with the buffer and dried under a vacuum. Protein was extracted and purified from ground samples using a developed phenol extraction method, followed by ammonium TCA-acetone precipitation (Zheng et al., 2013). The protein yield was determined by Bradford protein assay, using bovine serum albumin as a standard. The protein samples were stored at $-80\text{ }^{\circ}\text{C}$ before using.

2.5. iTRAQ labeling and SCX fractionation

Peptides were labeled with iTRAQ reagents according to the manufacturer's instructions (SCIEX Pte. Ltd, Framingham, MA, USA). Each aliquot (100 μg of peptide equivalent) was reacted with one tube of iTRAQ reagent. After the sample was dissolved in 100 μL of 0.05 M TEAB solution, pH 8.5, the iTRAQ reagent was dissolved in 41 μL of anhydrous acetonitrile. The mixture was incubated at room temperature for 1 h. Then 8 μL of 5% hydroxylamine were added to the sample and incubated for 15 min to quench the reaction. The Multiplex labeled samples were pooled and lyophilized. The iTRAQ-labeled peptides mixture was fractionated using a Strata X (C18, 3.5 μm , $2.1 \times 150\text{ mm}$) (Thermo Fisher Scientific, Waltham, MA, USA) on an LC-20AB HPLC pump system (Shimadzu Corporation, Kyoto, Japan) at 0.3 mL/min. Buffer A consisted of 10 mM ammonium formate and buffer B consisted of 10 mM ammonium formate with 90% acetonitrile; both buffers were adjusted to pH 10 with ammonium hydroxide. A total of 30 fractions were collected for each peptides mixture, and then concatenated to 15 (pooling equal interval RPLC fractions). The fractions were dried for nano HPLC-MS/MS analysis.

After vacuum drying, the sample (100 μg) was digested with trypsin (SCIEX Pte. Ltd, Framingham, MA, USA) at $37\text{ }^{\circ}\text{C}$ for 16 h. The tryptic peptides were reconstituted in 0.5 M TEAB and peptide labeling was performed by iTRAQ reagent (SCIEX Pte. Ltd, Framingham, MA, USA). After 2 h of labeling reactions, the peptides were further purified using Strata X C18 (Thermo Fisher Scientific, Waltham, MA, USA), the labeled peptide mixtures were then multiplexed and vacuum dried. Strong cation exchange (SCX) chromatography was performed with an LC-

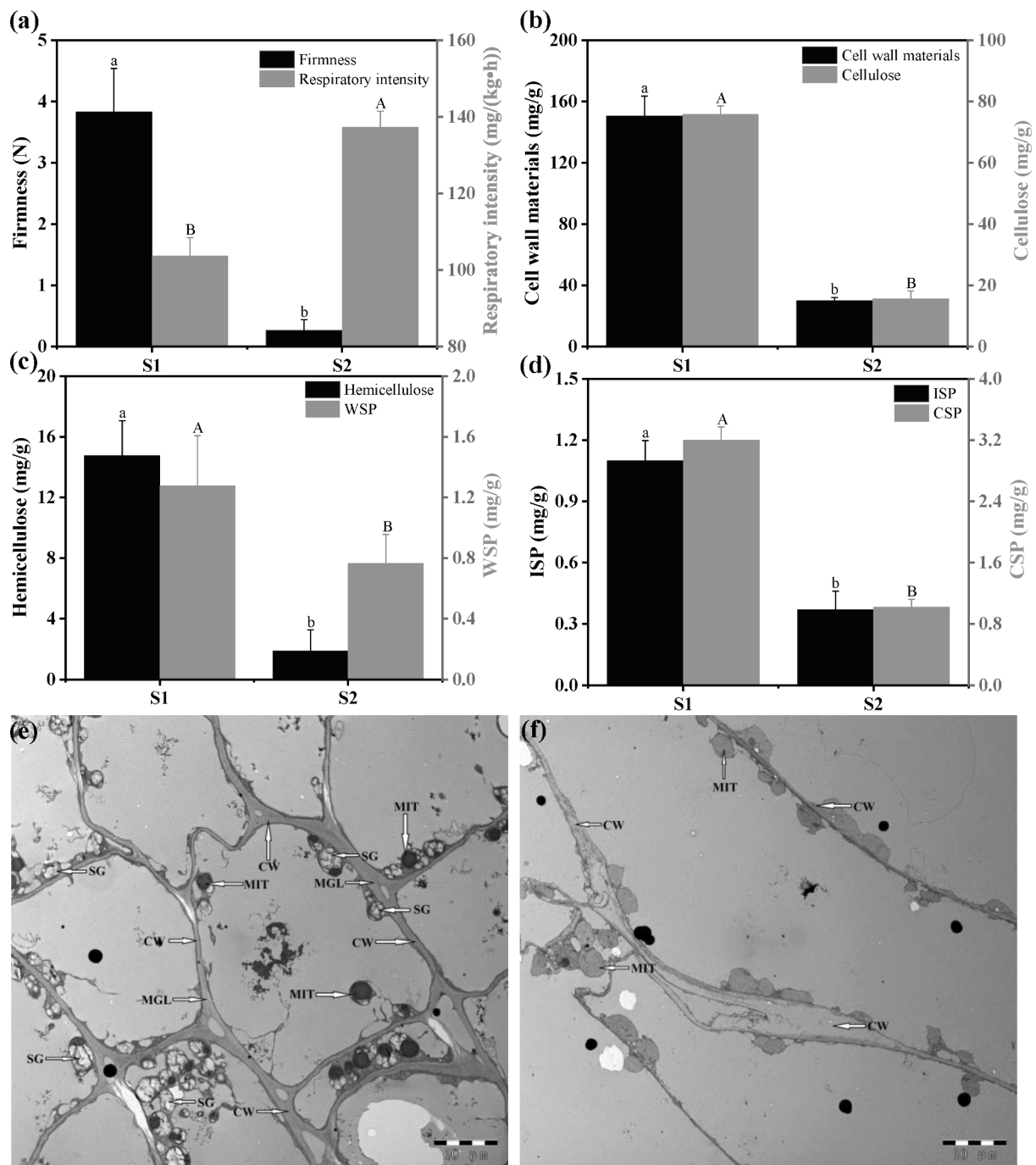


Fig. 1. (a) Changes in firmness and respiration rate of *Lycium barbarum* L. at stages S1 and S2. (b)–(d) Changes in cell wall component contents of harvested *Lycium barbarum* L. at different growing and ripening stages. (e) (f) TEM of thin-walled tissue of *Lycium barbarum* L. at stage S1. Different letters (a, b) (A, B) are significantly different ($P < 0.05$). (CWM) cell wall material; (WSP) water-soluble pectin; ISP, ionic soluble pectin; (CSP) covalent bound pectin; Scale bars indicate 5000 nm. (SG) Starch granule; (CW) Cell wall; (MGL) Mesothelium; (MIT) Mitochondria.

20AB HPLC pump system (Shimadzu Corporation, Kyoto, Japan).

2.6. HPLC-MS analysis

The peptide mixture (5 μg) was resuspended in buffer A (0.1% formic acid, 84% acetonitrile) and centrifuged for 10 min at 20,000 g, with the final concentration approximately 0.5 $\mu\text{g}/\mu\text{l}$. The mobile phase was acetonitrile and 0.1% formic acid-water solution, 10 μl supernatant was loaded onto an Easy LC HPLC (Thermo Fisher Scientific Inc, Waltham, MA, USA) by the autosampler onto a C18 trap column (Thermo Scientific EASY column, 10 cm, ID75 μm , 3 μm , C18-A2). The peptides were

then subjected to nanoelectrospray ionization, followed by tandem mass spectrometry (MS/MS) in a Q-Exactive system (Thermo Fisher Scientific Inc, Waltham, MA, USA) coupled online to the HPLC.

2.7. Bioinformatics analysis

Raw data were converted to RAW files for further bioinformatics analysis, and the exported RAW files were searched by the local Mascot server using the Mascot2.2 (Matrix Science Inc, London, UK) and Proteome Discoverer 1.4 (Thermo Fisher Scientific Inc, Waltham, MA, USA). To reduce the probability of false peptide identification, after a Mascot

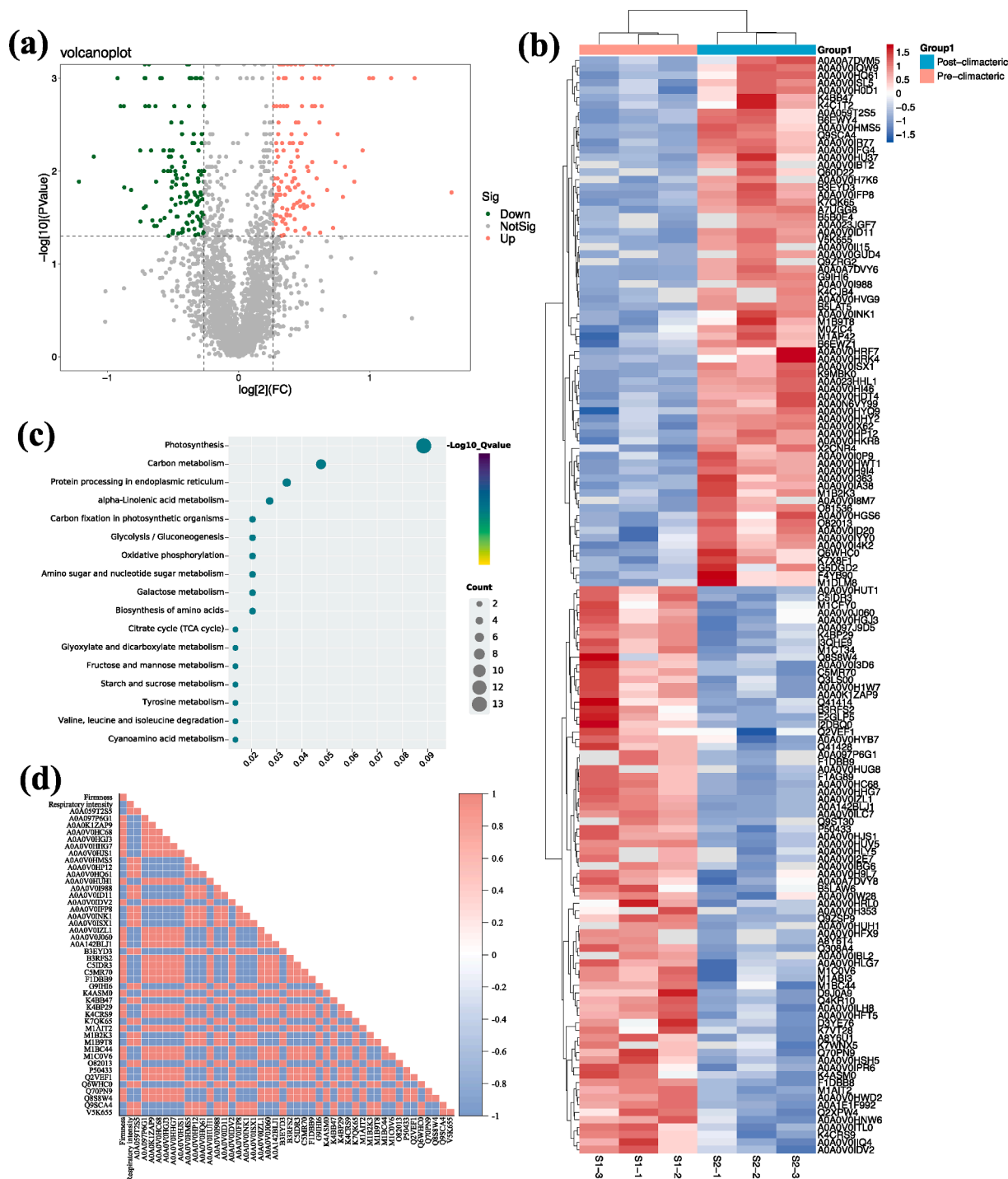


Fig. 2. (a) Volcano plot of significantly differentially accumulated proteins. (b) Heat map of clustering of differentially expressed proteins in S1 versus S2. (c) Bubble map of S1 and S2 KEGG pathway enrichment. (d) Spearman's correlation of fruit firmness and respiration rate and differentially expressed proteins in *Lycium barbarum* L. The x-axis is the fold change of differentially accumulated proteins expressed as Log2 and Y-axis is the corresponding -log10 (P-value). Fold changes ≥ 1.2 and t-test P-values < 0.05 were set as the threshold of significance for differential expression.

probability analysis using NCBI BLAST+ (NCBI-blast-2.2.28⁺-win32.exe), only those peptides at the E-value $\leq 1e-3$ confidence interval were counted as having been identified. Each protein identified with high confidence included at least two unique peptides. All proteins with a false discovery rate (FDR) $< 1\%$ were subjected to functional classification by the Clusters of Orthologous Groups of proteins UniProtKB (<https://www.uniprot.org>, FASTA database). Functional annotation and category analysis of the DEPs were performed using the online software Blast2GO Command Line (Version: go database_201608.obo download

address: <https://www.geneontology.org>). Furthermore, the COG database (<https://www.ncbi.nlm.nih.gov/COG/>) and KEGG database (<https://www.genome.jp/kegg/>) were used to classify the identified proteins.

2.8. Quantitative real-time PCR (RT-PCR) analysis

The RT-PCR experiment was conducted using an CFX fluorescent quantitative PCR instrument (Bio-Rad Laboratories, Richmond, CA,

Table 1
Quantification of DEPs (mean \pm SD) and fold change (FC) associated with fruit softening were screened for quantification.

	UniProt ID	Protein Name	S1	S2	P-value	Fold Change	
Photosynthesis and energy production	A0A097P6G1	Geranylgeranyl reductase	0.865 \pm 0.049	0.585 \pm 0.016	0.032	0.676	
	A0A0K1ZAP9	Photosystem II CP47 reaction center protein	0.860 \pm 0.060	0.597 \pm 0.038	0.006	0.694	
	A0A0V0HC68	Ribulose biphosphate carboxylase small chain	1.125 \pm 0.093	0.613 \pm 0.026	0.002	0.545	
	A0A0V0HGJ3	Putative oxygen-evolving enhancer protein 3, chloroplastic-like	0.744 \pm 0.044	0.573 \pm 0.059	0.030	0.770	
	A0A0V0HHG7	Cytochrome b6-f complex iron-sulfur subunit	0.894 \pm 0.049	0.636 \pm 0.017	0.002	0.712	
	A0A0V0HJS1	Cytochrome b559 subunit alpha	0.691 \pm 0.040	0.445 \pm 0.028	0.002	0.644	
	A0A0V0HP12	Succinate dehydrogenase [ubiquinone] iron-sulfur subunit, mitochondrial	1.254 \pm 0.045	1.563 \pm 0.041	0.002	1.246	
	A0A0V0HUH1	Aldose 1-epimerase	1.013 \pm 0.004	0.727 \pm 0.034	0.014	0.718	
	A0A0V0IFP8	Putative pyruvate decarboxylase 1-like	1.146 \pm 0.068	1.690 \pm 0.078	0.002	1.474	
	A0A0V0IZL1	Photosystem II D2 protein	0.812 \pm 0.051	0.428 \pm 0.022	0.001	0.527	
	A0A0V0J060	Putative photosystem I chlorophyll A apoprotein-like	0.805 \pm 0.057	0.614 \pm 0.066	0.037	0.763	
	A0A142BLJ1	ATP synthase subunit alpha, chloroplastic	0.827 \pm 0.016	0.630 \pm 0.013	0.000	0.762	
	B3RFS2	Chloroplast chlorophyll a/b-binding protein (Fragment)	0.951 \pm 0.130	0.629 \pm 0.062	0.034	0.661	
	C5MR70	Chloroplast manganese stabilizing protein-II (Fragment)	0.747 \pm 0.055	0.517 \pm 0.032	0.007	0.692	
	K4BB47	Succinate dehydrogenase [ubiquinone] flavoprotein subunit, mitochondrial	1.203 \pm 0.028	1.564 \pm 0.122	0.015	1.300	
	K4CRS9	Chlorophyll a-b binding protein, chloroplastic	0.565 \pm 0.053	0.308 \pm 0.072	0.015	0.546	
	M1B9T8	Aspartate aminotransferase	1.030 \pm 0.049	1.237 \pm 0.079	0.034	1.201	
	M1C0V6	Fructose-biphosphate aldolase	0.889 \pm 0.034	0.703 \pm 0.057	0.017	0.791	
	P50433	Serine hydroxymethyltransferase, mitochondrial	1.107 \pm 0.070	0.745 \pm 0.085	0.010	0.673	
	Q2VEF1	Photosystem II reaction center protein H	0.641 \pm 0.069	0.495 \pm 0.089	0.021	0.772	
	Q70PN9	Putative photosystem I reaction centre PSI-D subunit	0.581 \pm 0.039	0.435 \pm 0.031	0.014	0.748	
	Q8S8W4	Cytochrome <i>f</i>	0.853 \pm 0.117	0.698 \pm 0.036	0.039	0.819	
	Q9SCA4	Putative ferredoxin (Fragment)	1.036 \pm 0.024	2.110 \pm 0.181	0.001	2.036	
	Carbon biosynthesis and metabolism	A0A059T2S5	Sucrose-phosphate synthase	1.112 \pm 0.048	1.514 \pm 0.097	0.006	1.362
		A0A0V0HC68	Ribulose biphosphate carboxylase small chain	1.125 \pm 0.093	0.613 \pm 0.026	0.002	0.545
		A0A0V0HMS5	Putative tropinone reductase-like	1.010 \pm 0.037	1.704 \pm 0.164	0.004	1.687
A0A0V0HP12		Succinate dehydrogenase [ubiquinone] iron-sulfur subunit, mitochondrial	1.254 \pm 0.045	1.563 \pm 0.041	0.002	1.246	
A0A0V0HUH1		Aldose 1-epimerase	1.013 \pm 0.004	0.727 \pm 0.034	0.014	0.718	
B3EYD3		Chloroplast monodehydroascorbate reductase	1.187 \pm 0.008	1.517 \pm 0.056	0.001	1.278	
C5IDR3		Chitinase (Fragment)	0.674 \pm 0.050	0.500 \pm 0.028	0.012	0.742	
G9IHI6		Apoplastic invertase	1.178 \pm 0.013	1.888 \pm 0.063	0.000	1.603	
K4BB47		Succinate dehydrogenase [ubiquinone] flavoprotein subunit, mitochondrial	1.203 \pm 0.028	1.564 \pm 0.122	0.015	1.300	
K4BP29		Alpha-galactosidase	0.919 \pm 0.014	0.726 \pm 0.047	0.005	0.790	
M1AIT2		D-3-phosphoglycerate dehydrogenase	1.029 \pm 0.029	0.801 \pm 0.022	0.001	0.779	
M1B2K3		Phosphomannomutase	0.869 \pm 0.068	1.313 \pm 0.125	0.012	1.510	
M1B9T8		Aspartate aminotransferase	1.030 \pm 0.049	1.237 \pm 0.079	0.034	1.201	

(continued on next page)

Table 1 (continued)

	UniProt ID	Protein Name	S1	S2	P-value	Fold Change
	M1BC44	Beta-hexosaminidase	0.877 ± 0.014	0.724 ± 0.056	0.020	0.826
	M1C0V6	Fructose-bisphosphate aldolase	0.889 ± 0.034	0.703 ± 0.057	0.017	0.791
	P50433	Serine hydroxymethyltransferase, mitochondrial	1.107 ± 0.070	0.745 ± 0.085	0.010	0.673
Amino acids biosynthesis and metabolism	A0A0V0ID11	Putative 3-ketoacyl-CoA thiolase 2, peroxisomal-like	1.073 ± 0.034	1.448 ± 0.031	0.000	1.349
	F1DBB9	Chloroplast polyphenol oxidase	1.169 ± 0.078	0.741 ± 0.021	0.034	0.634
	K7QK65	Adenosylhomocysteinase	1.001 ± 0.022	1.256 ± 0.026	0.000	1.255
	M1AIT2	D-3-phosphoglycerate dehydrogenase	1.029 ± 0.029	0.801 ± 0.022	0.001	0.779
	M1B9T8	Aspartate aminotransferase	1.030 ± 0.049	1.237 ± 0.079	0.034	1.201
	M1C0V6	Fructose-bisphosphate aldolase	0.889 ± 0.034	0.703 ± 0.057	0.017	0.791
	P50433	Serine hydroxymethyltransferase, mitochondrial	1.107 ± 0.070	0.745 ± 0.085	0.010	0.673
Fatty acid biosynthesis and metabolism	A0A0K1ZAP9	Photosystem II CP47 reaction center protein	0.860 ± 0.060	0.597 ± 0.038	0.006	0.694
	A0A0V0I988	Putative fatty acid hydroperoxide lyase-like	1.178 ± 0.007	1.518 ± 0.003	0.002	1.289
	A0A0V0ID11	Putative 3-ketoacyl-CoA thiolase 2, peroxisomal-like	1.073 ± 0.034	1.448 ± 0.031	0.000	1.349
	A0A0V0IDV2	Putative allene oxide synthase-like	0.986 ± 0.069	0.691 ± 0.074	0.015	0.701
	K4ASM0	Lipoxygenase	0.905 ± 0.138	0.579 ± 0.065	0.039	0.640
	K4BP29	Alpha-galactosidase	0.919 ± 0.014	0.726 ± 0.047	0.005	0.790
Gene transcription translation and protein modification	A0A0V0HQ61	GTP-binding nuclear protein	1.143 ± 0.040	1.432 ± 0.087	0.013	1.253
	A0A0V0INK1	Putative ovule protein	1.147 ± 0.064	1.477 ± 0.126	0.030	1.287
	A0A0V0ISX1	Putative cell division cycle protein 48-like	1.025 ± 0.016	1.434 ± 0.055	0.001	1.399
	O82013	17.3 kDa class II heat shock protein	0.960 ± 0.048	1.416 ± 0.121	0.008	1.476
	Q6WHC0	Chloroplast small heat shock protein class I	0.881 ± 0.116	1.528 ± 0.212	0.019	1.734
	V5K655	Heat shock protein 70	1.054 ± 0.049	1.591 ± 0.048	0.000	1.510

USA), and the Solanales Actin gene (Gene symbol, LOC107840006) (Genomic Sequence: XM_016683691.1) was used as the internal reference gene. The $2^{-\Delta\Delta CT}$ method was used to calculate each gene's relative expression level (Liu et al., 2022). The corresponding gene primer sequences were presented in Table S1.

2.9. Statistical analysis

Experiments were performed in a completely randomized design with three replicates.

The analysis of statistically significant differences in firmness and cell wall components was performed by the independent samples *t*-test analysis at $P < 0.05$ using SPSS 24.0 software (SPSS Inc., Chicago, IL, USA). Graphs were constructed using Origin 2018 (OriginLab Inc., Northampton, Ma, USA).

3. Results and discussion

3.1. Changes in LBL firmness, cell wall fractions and microstructure

The reduction in firmness is considered to be a hallmark event of fruit

softening, and the measurements of firmness and physiological parameters in LBL allowed us to evaluate suitable materials to reveal the proteome changes associated with softening during ripening of LBL. Fruit firmness declined nearly 14-fold between the pre-climacteric (S1) (3.83 ± 0.71 N) and post-climacteric (S2) (0.27 ± 0.17 N) stages (Fig. 1a). As shown in Fig. 1a, fruit softening is accompanied by an increase in respiratory intensity and cell wall degradation. Fruit respiratory intensity increased from 103.80 ± 4.65 mg/(kg·h) at S1 to 137.33 ± 4.18 mg/(kg·h) at S2, with a percentage increase of 32.30%. Parenchyma tissues of LBL were extensively altered from S1 to S2. The contents of cell wall components, including protopectins (WSP, CSP and ISP), cellulose and hemicellulose, showed significant decreases ($P < 0.05$) (Fig. 1b, c). These cell wall materials structurally support cells and organs, and their solubilization or depolymerization may alter cell wall structure and cell-to-cell adhesion. The parenchyma tissue and cell wall were intact at the S1 stage, but as the ripening progressed, they underwent a large deformation, particularly at the S2 stage (Fig. 1e, f), indicating that the progressive changes of cell microstructure may be caused by the breakage and separation of the cell wall. In summary, this reduction or disappearance of structural cell wall material, which did not provide strong support for cells and tissues, led to a reduction in fruit

firmness. However, further analysis of the metabolic processes involved in cell wall degradation is required.

3.2. Protein identification, quantification and expression profiles

To identify the key proteins associated with the modification of cell wall components, structures and function, we sampled S1 and S2 before harvest, corresponding to fruits at the post-climacteric and post-climacteric stages, respectively, for comparative analysis of the LBL fruit cell wall proteome using iTRAQ technology. Extraction and identification of S1 and S2 cell wall proteins resulted in the identification of 2811 cell wall proteins (Table S2). Protein abundance values of $P < 0.05$ and fold change (FC) > 1.2 were considered to be significantly different between the S1 and S2. The volcano plot revealed the asymmetry of differentially expressed proteins (DEPs) between up-regulated and down-regulated proteins (Fig. 2a). Two hundred and eighty-five proteins were identified as DEPs (Fig. 2b), and the clustering heat map showed the clustering of the DEPs, with the two groups of samples showing good intra-group similarity and inter-group variability. The heat map also showed that 133 and 125 proteins were up-regulated and down-regulated at S1 and S2 respectively. Previous studies (Jiang et al., 2020; Jiang, Feng, Zhang, Luo, & Yu, 2020) reported that the process of fruit softening was related to energy production and conversion, amino acid transport and metabolism, carbohydrate metabolism, cell wall/membrane, and secondary metabolism. Hence, we further analysed the involvement of these DEPs in the metabolic processes associated with fruit softening.

A total of 147 proteins were involved in the physiological regulation of fruit by enriching the screened DEPs into the KEGG pathway (Table S2). Excluding uncharacterised proteins, 44 DEPs were correlated with fruit softening by their involvement in metabolic processes, including photosynthesis and energy production, carbon biosynthesis and metabolism, amino acids biosynthesis and metabolism, fatty acid biosynthesis and metabolism, gene transcription translation and protein modification and redox regulation (Table 1, Fig. 2c). The correlation of these 44 DEPs with fruit softening was analysed using Spearman correlations (Fig. 2d). As expected, these proteins showed a clear association with firmness. This may also verify that the metabolic processes involved in these proteins lead to fruit softening. Of these, 23 proteins were involved in the process of photosynthesis and energy production, mainly associated with the photosystem, chloroplast and cytochromes. The down-regulation of these proteins indicates a reduced photosynthesis, and that the fruit may ripe and soften.

Metabolic activity is dominated by carbohydrates, amino acids and fatty acids metabolism. Jiang et al. (2020) reported that the metabolism of amino acids and fatty acids produced the flavour and aromatic substances of the fruit and was not directly related to fruit softening. In contrast, the metabolism of carbohydrate compounds was thought to be the underlying cause of fruit softening. Carbohydrates are the basic substances for fruit energy metabolism and storage, as well as the basic skeletal unit of fruit and tissues (Wang et al., 2021), and glycan degradation leads to a weakening of the cell wall support, resulting in fruit softening. The β -hexosaminidase involved in glycan degradation is responsible for the degradation of glycans by hydrolyzing β -N-acetylamino glucose or β -N-acetylamino galactose at the ends of glycosides, oligosaccharides, polysaccharides and complex sugars (e.g. glycolipids, glycoproteins) (He et al., 2017). However, the synergistic action of cell wall degrading enzymes, including α -galactosidase, β -galactosidase, pectate lyase and pectinesterase is known to promote the degradation and depolymerisation of cell wall materials. In this study, although some of the cell wall degrading enzymes were identified (Table S1), the differences in their protein expression levels were not significant at the S1 and S2 stages. Degradation of the cell walls is necessitated by a combination of enzymatic reactions, and the lack of significant differences in their expression levels suggests that the abundance of these cell wall degrading enzymes remains at high levels. Recent works have shown

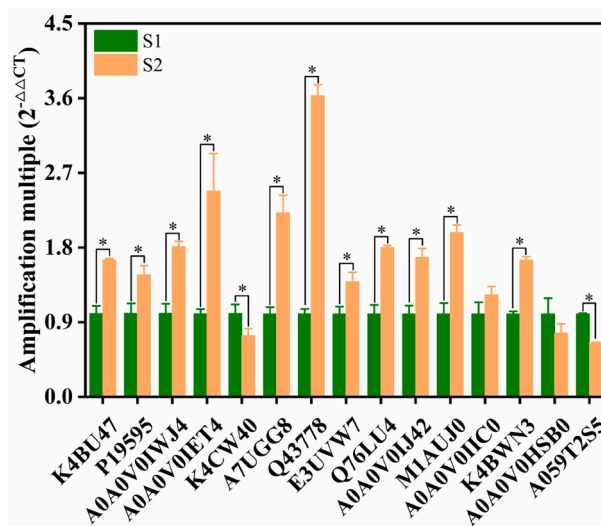


Fig. 3. Identification of gene expression of differentially expressed proteins associated with *Lycium barbarum* L. fruit softening. The values with “*” are significantly different ($P < 0.05$). K4BU47, Glucose-6p isomerase; P19595, Glucose-1-phosphate phosphodismutase; A0A0V0IWJ4, Aconitate hydratase; A0A0V0IET4, Citrate synthase; K4CW40, Malate dehydrogenase; K4BVK9, Endoglucanase; Q43778, β -glucosidase; E3UVW7, β -galactosidase; Q76LU4, α -L-arabinofuranosidase; A0A0V0IJ42, Pectinesterase; M1AUJ0, α -galactosidase; A0A0V0IIC0, Pectate lyase; K4BWN3, α -amylase; A0A0V0HSB0, β -amylase; A059T2S9, Sucrose-phosphate synthase.

that the softening of fruit was closely linked to the degradation of starch (Zhu et al., 2021). Starch, the glycogen of the plant, is the first to be broken down during carbohydrate metabolism. As shown Fig. 1, the starch granules disappeared at the S2 stage, suggesting that the degradation of polysaccharides was converted from glycogen to structural polysaccharides.

3.3. Gene expression of proteins associated with fruit softening

Next, RT-PCR was used to verify the mRNA expression of the proteins associated with cell wall degradation (Fig. 3). Except for pectate lyase, polygalacturonase, pectate lyase, pectinesterase, α -galactosidase, β -galactosidase and α -arabinofuranosidase were significantly up-regulated. The mRNA expression levels of α -amylase and β -amylase involved in starch degradation were higher in S2 than S1. Pectinesterase can remove the methoxyl group in the carboxyl residues present in pectin and catalyzes the conversion of pectin ester acid to pectin acid, which can then be degraded by pectinesterase. In addition, α -galactosidase hydrolyses the terminal, non-reducing alpha-D-galactose residues in alpha-D-galactosides, including galactose oligosaccharides, galactomannans and galactolipids, β -galactosidase cleaves the β -D-galactose residue in the side chain of rhamnogalacturonan I type pectin, and the two together promote the hydrolysis of pectin (Wen, Ström, Tasker, West, & Tucker, 2013). The contents of crude cell wall materials, cellulose, hemicellulose and pectin (WSP, ISP, CSP) significantly decreased in the S2 compared to the S1 (Fig. 1). This is consistent with a previous study (Liu et al., 2021), and suggests that exploring the reasons for the reduction in cell wall materials is important in revealing fruit softening. In addition, glucose-6p isomerase, glucose-1-phosphate phosphodismutase, aconitate hydratase, citrate synthase, malate dehydrogenase and β -glucosidase involved in glycolysis/gluconeogenesis, pentose phosphate pathway, pyruvate metabolism, citrate cycle (tca cycle) energy metabolism processes, were also significantly up-regulated ($P < 0.05$). The weakening of photosynthesis and the enhancement of respiration may lead to the depletion of macromolecules. As shown in Fig. 1a and Table 1, the fruit had a weakened energy synthesis during the S2

period and an enhanced energy metabolic activity, including the cell wall, starch, and other glycans being broken down and consumed as respiratory substrates, which weakened or even eliminated the cellular support structures, leading to softening of the fruit.

4. Conclusions

The degradation of cell wall components during fruit ripening is an intrinsic factor of LBL fruit softening, which was verified by the micro-structure of the fruit tissue. The iTRAQ technology was used to identify 258 differentially expressed cell wall proteins (DEPs) when fruit underwent the transition from the mature pre-climacteric (S1) to the post-climacteric (S2) stage. The DEPs were related to photosynthesis and energy production, carbon biosynthesis and metabolism, amino acids biosynthesis and metabolism, fatty acid biosynthesis and metabolism, gene transcription/translation and protein modification, which were implicated in LBL fruit softening. Fruit softening was caused by cell wall degradation, where energy metabolism caused large molecules of cell wall materials to be broken down into substrates for respiratory metabolism, and the gene expression of these enzymes was verified using RT-PCR. The identification of these proteins and pathways associated with cell wall degradation may provide a good starting point for further dissection of the molecular mechanisms underlying LBL fruit softening.

Declaration of Competing Interest

The authors declare that they have no known competing financial interests or personal relationships that could have appeared to influence the work reported in this paper.

Acknowledgments

We thank Dr. Hao Xu of Jiangnan University for his help in the project idea and experimental process. We are grateful to lecturer Yuhui Zhao of Shizuishan Institute of Industry and Trade for her fundamental work in the early stage of this study. We thank Associate Professor Yanli Fan from the School of Food and Wine, Ningxia University for providing the instruments. Thanks to the National Natural Science Foundation of China (Project No. 31560436) for funding this research.

Funding

This research was entirely funded by the National Natural Science Foundation of China (Project No. 31560436).

Data availability statement

Research data are not shared.

Appendix A. Supplementary data

Supplementary data to this article can be found online at <https://doi.org/10.1016/j.fochms.2022.100110>.

References

- Bashline, L., Lei, L., Li, S., & Gu, Y. (2014). Cell wall, cytoskeleton, and cell expansion in higher plants. *Molecular Plant*, 7, 586–600. <https://doi.org/10.1093/mp/ssu018>
- Blumenkrantz, N., & Asboe-Hansen, G. (1973). New method for quantitative determination of uronic acids. *Analytical Biochemistry*, 54, 484–489. [https://doi.org/10.1016/0003-2697\(73\)90377-1](https://doi.org/10.1016/0003-2697(73)90377-1)
- Chea, S., Yu, D. J., Park, J., Oh, H. D., Chung, S. W., & Lee, H. J. (2019). Fruit softening correlates with enzymatic and compositional changes in fruit cell wall during ripening in 'Bluecrop' highbush blueberries. *Scientia Horticulturae*, 245, 163–170. <https://doi.org/10.1016/j.scienta.2018.10.019>
- D'Amour, J., Gosselin, C. J., Arul, J., Staigne, F. C., & Willemot, C. (2006). Gamma radiation affects cell wall composition of strawberries. *Journal of Food Science*, 58, 182–185. <https://doi.org/10.1111/j.1365-2621.1993.tb03239.x>
- Defilippi, B. G., Ejsmentewicz, T., Covarrubias, M. P., & Gudenschwager, O. (2018). Changes in cell wall pectins and their relation to postharvest mesocarp softening of Hass avocados (*Persea americana* Mill.). *Plant Physiology and Biochemistry*, 128, 142–151. <https://doi.org/10.1016/j.plaphy.2018.05.018>
- Gong, X., Bao, J., Chen, J., Qi, K., Xie, Z., Rui, W., ... Tao, S. (2020). Candidate proteins involved in the calyx abscission process of 'Kuerlexiangli' (Pyrus sinkiangensis Yu) identified by iTRAQ analysis. *Acta Physiologiae Plantarum*, 42, 112. <https://doi.org/10.1007/s11738-020-03097-x>
- Goulao, L. F., & Oliveira, C. M. (2008). Cell wall modifications during fruit ripening: When a fruit is not the fruit. *Trends in Food Science & Technology*, 19, 4–25. <https://doi.org/10.1016/j.tifs.2007.07.002>
- Guo, X., Xu, J., Cui, X., Chen, H., & Qi, H. (2017). iTRAQ-based protein profiling and fruit quality changes at different development stages of oriental melon. *Bmc Plant Biology*, 17, 28. <https://doi.org/10.1186/s12870-017-0977-7>
- Gwanpua, S. G., Verlinden, B. E., Hertog, M., Nicolai, B. M., & Geeraerd, A. (2017). A transcriptomics-based kinetic model for enzyme-induced pectin degradation in apple (*Malus × domestica*) fruit. *Postharvest Biology and Technology*, 130, 64–74. <https://doi.org/10.1016/j.postharvbio.2017.04.008>
- He, X., Li, L., Sun, J., Li, C., Sheng, J., Zheng, F., ... Tang, Y. (2017). Adenylate quantitative method analyzing energy change in postharvest banana (*Musa acuminata* L.) fruits stored at different temperatures. *Scientia Horticulturae*, 219, 118–124. <https://doi.org/10.1016/j.scienta.2017.02.050>
- Jiang, L., Feng, L., Zhang, F., Luo, H., & Yu, Z. (2020). Peach fruit ripening: Proteomic comparative analyses of two cultivars with different flesh texture phenotypes at two ripening stages. *Scientia Horticulturae*, 260, Article 108610. <https://doi.org/10.1016/j.scienta.2019.108610>
- Jiang, L., Kang, R., Feng, L., Yu, Z., & Luo, H. (2020). iTRAQ-based quantitative proteomic analysis of peach fruit (*Prunus persica* L.) at different ripening and postharvest storage stages. *Postharvest Biology and Technology*, 164, Article 111137. <https://doi.org/10.1016/j.postharvbio.2020.111137>
- Liu, D., Liu, J., Li, P., & Zhao, X. (2020). Development status and research progress of deep processing products of *lycium barbarum*. *Journal of Food Science and Technology (China)*, 38, 10–20. <https://doi.org/10.3969/j.issn.2095-6002.2020.04.002>
- Liu, J., Liu, D., Wu, X., Pan, C., Wang, S., & Ma, L. (2022). TMT quantitative proteomics analysis reveals the effects of transport stress on iron metabolism in the liver of chicken. *Animals*, 12, 52. <https://doi.org/10.3390/ani12010052>
- Liu, Y., Tang, M., Liu, M., Su, D., Chen, J., Gao, Y., ... Li, Z. (2020). The molecular regulation of ethylene in fruit ripening. *Small Methods*, 4, 1900485. <https://doi.org/10.1002/smt.201900485>
- Liu, J., Zhao, Y., Xu, H., Zhao, X., Tan, Y., Li, P., ... Liu, D. (2021). Fruit softening correlates with enzymatic activities and compositional changes in fruit cell wall during growing in *Lycium barbarum* L. *International Journal of Food Science & Technology*, 56, 3044–3054. <https://doi.org/10.1111/ijfs.14948>
- Martinez-Esteso, M. J., Sellés-Marchart, S., Vera-Urbina, J. C., Pedreño, M. A., & Bru-Martinez, R. (2009). Changes of defense proteins in the extracellular proteome of grapevine (*Vitis vinifera* cv. Gamay) cell cultures in response to elicitors. *Journal of Proteomics*, 73, 331–341. <https://doi.org/10.1016/j.jprot.2009.10.001>
- Martinez-Esteso, M., Vilella-Antón, M., Pedreño, M. A., Valero, M. L., & Bru-Martinez, R. (2013). iTRAQ-based protein profiling provides insights into the central metabolism changes driving grape berry development and ripening. *BMC Plant Biology*, 13, 167. <https://doi.org/10.1186/1471-2229-13-167>
- Niu, J., Cao, D., Li, H., Xue, H., Chen, L., Liu, B., & Cao, S. (2018). Quantitative proteomics of pomegranate varieties with contrasting seed hardness during seed development stages. *Tree Genetics & Genomes*, 14, 14. <https://doi.org/10.1007/s11295-018-1229-1>
- Ricardo, N. P., Campos-Vargas, R., & Orellana, A. (2012). Assessment of *Prunus persica* fruit softening using a proteomics approach. *Journal of Proteomics*, 75, 1618–1638. <https://doi.org/10.1016/j.jprot.2011.11.037>
- Wang, H., Cheng, X., Wu, C., Fan, G., Li, T., & Dong, C. (2021). Retardation of postharvest softening of blueberry fruit by methyl jasmonate is correlated with altered cell wall modification and energy metabolism. *Scientia Horticulturae*, 276, Article 109752. <https://doi.org/10.1016/j.scienta.2020.109752>
- Wen, B., Ström, A., Tasker, A., West, G., & Tucker, G. A. (2013). Effect of silencing the two major tomato fruit pectin methylesterase isoforms on cell wall pectin metabolism. *Plant Biology*, 15, 1025–1032. <https://doi.org/10.1111/j.1438-8677.2012.00714.x>
- Xiao, L., Li, T., Jiang, G., Jiang, Y., & Duan, X. (2019). Cell wall proteome analysis of banana fruit softening using iTRAQ technology. *Journal of Proteomics*, 209, Article 103506. <https://doi.org/10.1016/j.jprot.2019.103506>
- Zheng, Q., Song, J., Campbell-Palmer, L., Thompson, K., Li, L., Walker, B., ... Li, X. (2013). A proteomic investigation of apple fruit during ripening and in response to ethylene treatment. *Journal of Proteomics*, 93, 276–294. <https://doi.org/10.1016/j.jprot.2013.02.006>
- Zhu, L., Shan, W., Wu, C., Wei, W., Xu, H., Lu, W., ... Kuang, J. (2021). Ethylene-induced banana starch degradation mediated by an ethylene signaling component MaEIL2. *Postharvest Biology and Technology*, 181, Article 111648. <https://doi.org/10.1016/j.postharvbio.2021.111648>